Wavelike Motion of a Mechanical Vocal Fold Model at the Onset of Self-Excited Oscillation*

Shinji DEGUCHI**, Yusuke MIYAKE**, Yoshihiko TAMURA**, and Seiichi WASHIO**

**Graduate School of Natural Science and Technology, Okayama University
Tsushima-naka 3-1-1, Okayama 700-8530, Japan
E-mail: deguchi@mech.okayama-u.ac.jp

Abstract

The vocal folds in the larynx experience a self-excited oscillation with a wavelike motion during speech owing to interaction with respiratory airflow. The mechanism of the onset of the oscillation remains elusive partly because of compound effects of laryngeal muscles, although its better understanding has clinical significance in determining the ease with which phonation can be achieved. Approaches to the mechanism using a mechanical vocal fold model are useful because it allows investigating the roles of interested parameters in isolation. Here, we designed a mechanical vocal fold model made of a pair of rubber sheets. A key feature of the experimental setup is that it enables observations of high-speed deformation of the oscillating vocal fold model, together with pressure evaluations while changing separately isolated parameters associated with the laryngeal muscle functions. The observations of the oscillation onset demonstrated a gradually developed wavelike oscillation that spreads out over the rubber sheets. The magnitude of the motion is restricted by either increase in rubber restoring force or reduction in flow path width, each of the effects mimics the actual laryngeal muscle functions and reduces, in the experimental results, the threshold upstream pressure that induces the onset of the self-excitation. Thus, the present study highlights close association between degrees of oscillation, flow-tissue interaction, and threshold pressure required for the onset.

Key words: Self-excited Oscillation, Flow-Structure Interaction, High-Speed Video Camera, Pressure Measurement, Vocal Fold, Airway, Phonation

1. Introduction

Self-excited oscillation of the vocal fold caused by interactions between its deformation and respiratory airflow makes a major sound source of human voiced speech [1-4]. It is expected that understanding of details of the vocal fold oscillation mechanism elucidates the optimum mechanical conditions at which the oscillation is most likely to occur. This knowledge will contribute to clinical applications such as development of treatment for voice disorders and design of artificial larynx [5].

The oscillation mechanism actually remains elusive partly because of the complexity of the larynx system controlled by laryngeal muscles [6]. The vocal folds form a constriction in the airway by using a pair of mucosal projections with the help of the related muscles to become suitable for the flow-tissue interaction. Some of the muscles also alter tension level in the vocal fold tissue. Thus, the geometry and biomechanical properties of the vocal folds, both of which affect the voice pitch, are simultaneously controlled by the activations of the muscles involved. This restriction makes the interpretation of measurement results on

human subjects difficult. Specifically, it is ambiguous how each of those factors, e.g. tension level and geometry, has a dominant influence on the voice pitch control, although it has been reported that the phonation becomes increasingly harder as the voice pitch is raised within the modal phonation [7].

Approaches to the mechanism using a mechanical vocal fold model are therefore useful because it enables to investigate the roles of interested parameters in isolation. Titze et al. [8, 9] examined the threshold values of an upstream pressure, which trigger self-excited oscillations of a mechanical vocal fold model made of a fluid-encapsulated silicone membrane. The upstream pressure models the human lung pressure that provides the source energy for inducing the self-excited oscillation of the vocal folds. In the model, a flow path width formed by a unilateral constriction holding the silicone membrane was altered by regulating the position of the constriction. However, this system may allow leaking air, which results in inaccuracy of the measurement. In addition, the mechanical properties of the vocal fold model were altered by changing the viscosity of the encapsulated fluid. This modeling, however, seems to lack the ability of controlling lateral tension in the membrane, which has a considerable influence on the voice pitch control [6] as well as the ease of phonation [5, 7]. Another methodological issue of particular importance is that the oscillatory pattern of the vocal fold model was not checked in the past studies. Accordingly, deformation-related parameters, which will be vital for considering the vocal fold mechanics, such as the magnitude of amplitude, the effects of collisions between the facing vocal folds, and the fundamental frequency of the oscillation were not highlighted.

The actual vocal folds exhibit a motion called a mucosal wave during speech according to in vivo observations using a high-speed camera or a laryngo-stroboscopy [2, 5, 10]. The term, mucosal wave, is named since a 1- to 2-mm thickness surface layer that constitutes the vocal fold mucosa propagates a surface wave along the glottis in the direction of airflow at a fundamental frequency of >100 Hz. The in vivo observation techniques allow viewing the vocal folds from only above, which is unsuitable for obtaining a full and exact picture of the wavelike motion that moves periodically from the bottom to the top. Hence, it is a good approach to establish a model of the mucosal wave, to view it from a lateral direction for exact evaluations of the behaviors such as its amplitude or collision, and to investigate how biomechanical factors affect the motion making the sound source.

In the present study, we newly design a mechanical vocal fold model made of a pair of rubber sheets. A key feature of the experimental setup is that it enables observations of the deformation of the oscillating vocal fold model from arbitrary directions including a lateral direction, together with pressure evaluations while changing separately two isolated parameters, i.e. restoring force in the vocal fold model and initial width of the vocal fold model constriction. Here, we focus in particular on oscillatory patterns at the onset of self-excited oscillations of the vocal fold model. Thus, we expect to assess, in terms of the direct observation, the roles of the laryngeal muscles in the initiation of the self-excitation.

Nomenclature

X_c: Position of the minimum gap point in the constriction

X_u: Position of 9-mm upstream of X_c

A_c: Initial cross-sectional area at X_c

F_0: Fundamental frequency of the rubber oscillation

P_t: Pressure at the inlet tank

P_u: Pressure at X_u

P_c: Pressure at X_c

P_{th}: Threshold pressure of P_t required to induce the onset of the rubber oscillation

T_l: Initial tension in the lateral direction of the rubber sheets

2. Methods

2.1 Experimental setup

An experimental flow path was constructed on a vibration-free table that mimics a part of the human airway (Fig. 1a). It consists of a pressure tank placed at the uppermost stream inlet and a constriction placed at the exit, both of which are connected to each other through a rectangular straight flow path that copies the trachea in the airway and has a longitudinal (X) length of 250 mm, a height (Z) of 16 mm, and a depth (Y, a direction perpendicular to the sheet) of 20 mm. The tank having a volume of 10^{-1} m^3 is pressurized at a rate of ~0.25 kPa/s by manually opening a release valve of a compressor during experiments to provide airflow to the flow path like the lungs provide respiratory flow to the airway in the human phonation. The constriction is formed by a pair of curved walls to have a shape similar with the actual vocal folds (Fig. 1b). Each curved wall consists of a single silicone rubber sheet with a thickness of 0.2 mm. The other side space of the sheet opposite to the flow path side is hollow and is opened to the air. The rubber sheet is sustained at all four rigid sides while keeping the vocal fold-like shape. The overall flow path is sealed except for the exit of the flow path that is 20-mm away from the constriction exit and is opened to the air. One of the rigid side-wall in the X-Z plane is made of transparent acrylic, thereby allowing to observe a deformation of the rubber sheet from the outside. The other rigid side-wall made of duralumin consists of three separate pieces. One of the separate pieces has an hourglass-shaped constricted form, and the geometry of the constriction is the same with the vocal fold-like shape described above. Each of the other two has the vocal fold-like shape at its one end to be faced to the hourglass-shaped piece. Thus, incorporation of the separate components into one makes a rectangular form having two thin slits, into which the rubber sheets are inserted to form the vocal fold-like shape. In the outer side of the duralumin wall, a force-gauge is mounted, which stretches one ends of the rubber sheets to regulate lateral (Y-direction) tension level (hereafter referred to as T_l) in the sheets prior to experiment. Accordingly, T_l can be regulated without both air leakage and change in the length of the flow path depth, imitating the role of the crycothyroid muscle activation in the actual human larynx for control of voice pitch [6]. In order to imitate the role of the arytenoid cartilage that controls width of the glottis [6], a thin bolt is mounted inside each of the sheets. Regulation of the position of the bolts pushes a part of the end of the sheets at the minimum gap points (X_c) toward the center of the flow path and narrows the distance between the sheets, thereby controlling the initial gap width. Since the depth of the flow path, 20 mm, is constant, and the cross-section of the constriction has a triangular shape, the initial cross-sectional area at X_c (A_c) is proportional to the gap width. Pressure transducers (PD104KW, JTEKT) hooked up to DC amplifiers were embedded in the rigid acrylic side-wall at X_c and its 9-mm front (X_u) to measure pressure fluctuations P_c and P_u, respectively, and record the data on a computer. Pressures were also measured at the inlet tank (P_t), which models a pressure in the human lungs.

2.2 Measurement of oscillation onset pressure

Application of pressure on the inlet tank produces airflow in the flow path. A self-excited oscillation of the rubber sheets occurs when P_t reaches a threshold value. After the onset of the oscillation, we ceased the pressurization. P_t was then gradually decreased, and the self-excited oscillation finally stopped being maintained. Time course changes in the pressures during the process (i.e., the oscillation onset and stop) were recorded on the computer. The threshold pressure P_{th} was obtained from the data, which is defined as the inlet tank pressure P_t where the oscillation starts. P_{th} thus models the minimum lung pressure required for phonation. P_{th} was measured at various combinations of T_l and A_c. The magnitude of T_l ranges from 0.0 N to 2.0 N at a 0.5-N interval. The 0.0-N force means that no initial tension exists in the rubber sheets. The magnitude of A_c ranges from 10 mm^2 to 30
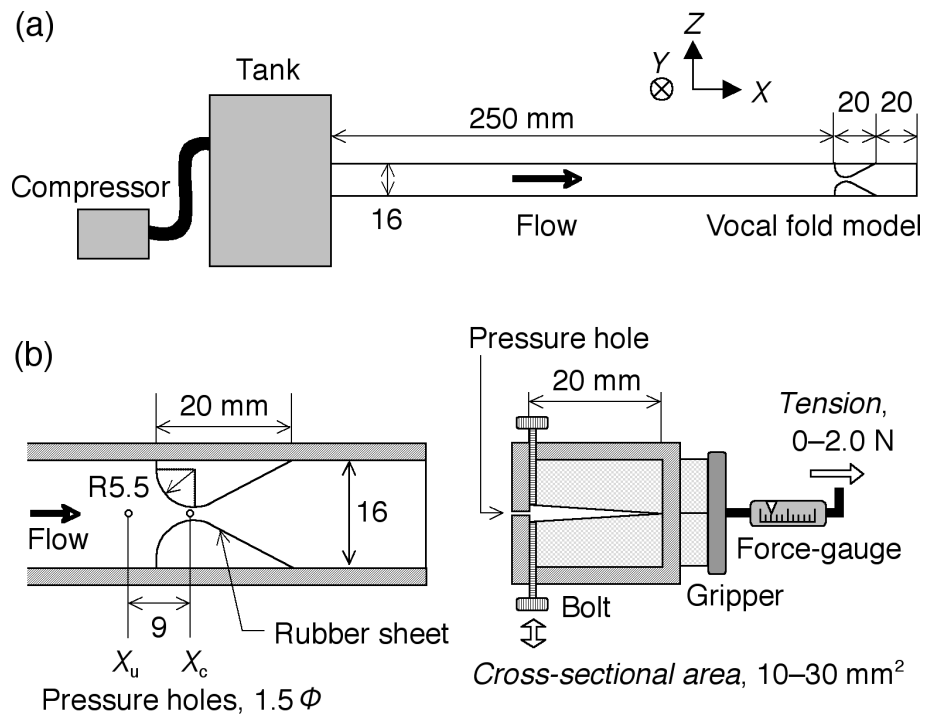
Fig. 1 Schematic diagram of the airway model. (a) Overall view. (b) Detail of vocal fold model.

mm^2 at a 5-mm^2 interval. Fundamental frequency and intensity of the fluctuation of P_c immediately after the oscillation onset were also measured for the various combinations of the parameters.

2.3 High-speed video camera observation

A high-speed video camera (HCV-1, Shimadzu) was used to observe detailed behaviors of the rubber sheets during the oscillation at an 8000-frames per second shutter speed. In the observation of the *X-Z* plane, the pressure measurements were not simultaneously done because existence of the pressure transducers that lie in the acrylic side-wall of the constriction interferes the camera view. Alternatively, the side-wall is replaced by another one without pressure holes, and a condenser microphone hooked up to an amplifier was placed near the downstream exit. A sound generated by the rubber oscillation was detected by this microphone, and an electric circuit linked to the amplifier converted the detected voltage into a trigger pulse voltage signal for precise synchronization of the image capture using the camera with the instant of the initiation of the rubber oscillation.

3. Results

3.1 Oscillation onset pressure

Before the pressure measurement experiment, we preliminarily observed self-excited oscillation of the vocal fold model by using a normal CCD video camera (DM-FV M20, Canon) with a frame frequency of 30 Hz. As the inlet tank was compressed, airflow was gradually generated in the flow path. The observation from the lateral direction showed that the central portions of the rubber sheets were then deformed toward the downstream owing to the loading of the pressure (Figs. 2a and b). The rubber sheets finally started to oscillate and produced a buzzing sound when P_t had reached a threshold value (i.e., P_{th}) (Fig. 2c). Immediately after the initiation of the oscillation, we stopped compressing the inlet tank. This resulted in that the rubber sheets eventually stopped oscillating and returned to their

original position and shape (Fig. 2d).

The pressure measurement was done during the above-mentioned process (Fig. 3a). Time course changes in the pressures at a lateral tension T_l of 0.0 N and a cross-sectional area A_c of 30 mm^2, as a typical result, demonstrated that the amplitudes of the pressure fluctuations became considerably larger when P_t reached 1.7 kPa, which is defined as P_{th}. Magnification of the pressures–time relation (Fig. 3b) reveals that the fluctuation is periodical and has a fundamental frequency of 320 Hz. Since we ceased to compress the inlet tank after the oscillation onset, P_t was gradually reduced thereafter. We found that the rubber sheets keep oscillating even when P_t falls to below P_{th}, indicating that the inlet pressure required for sustaining the self-excited oscillation is lower than that for triggering its onset. In the case of Fig. 3a, the oscillation attenuated at last when P_t reached 1.3 kPa. We confirmed from qualitative and quantitative viewpoints the repeatability of the phenomena found in the experiment.

The threshold value P_{th} was obtained at parametric combinations of T_l and A_c (Fig. 4a). Magnitude of P_{th} shown as a function of T_l and A_c reveals that it has a larger value of ~3.3
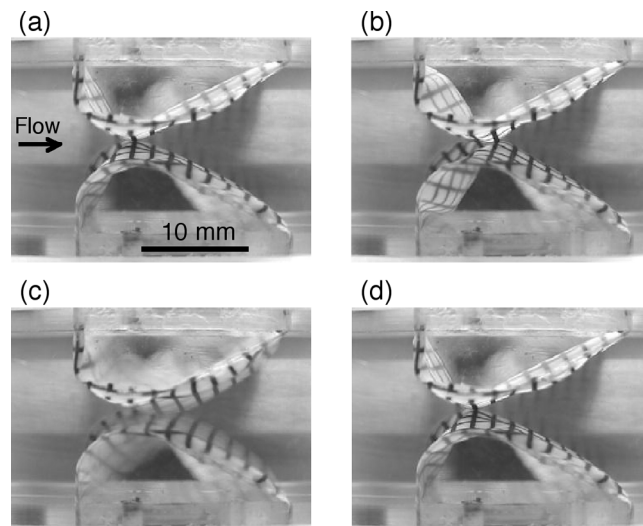

Fig. 2 Images of a rubber oscillation in the *X-Z* plane taken by the normal CCD video camera. (a) Initial. (b) Immediately before an onset of a self-excited oscillation. (c) Just after a stop of the oscillation. (d) Just after a cessation of the oscillation.
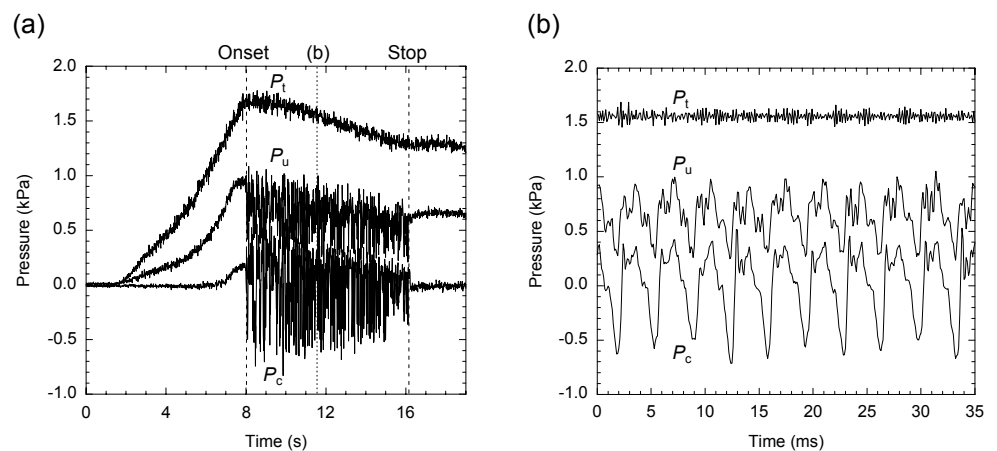

Fig. 3 Pressure fluctuations during the experiment of T_l = 0.0 N and A_c = 30 mm^2. (a) Whole time course. (b) Magnified data after the oscillation initiation.
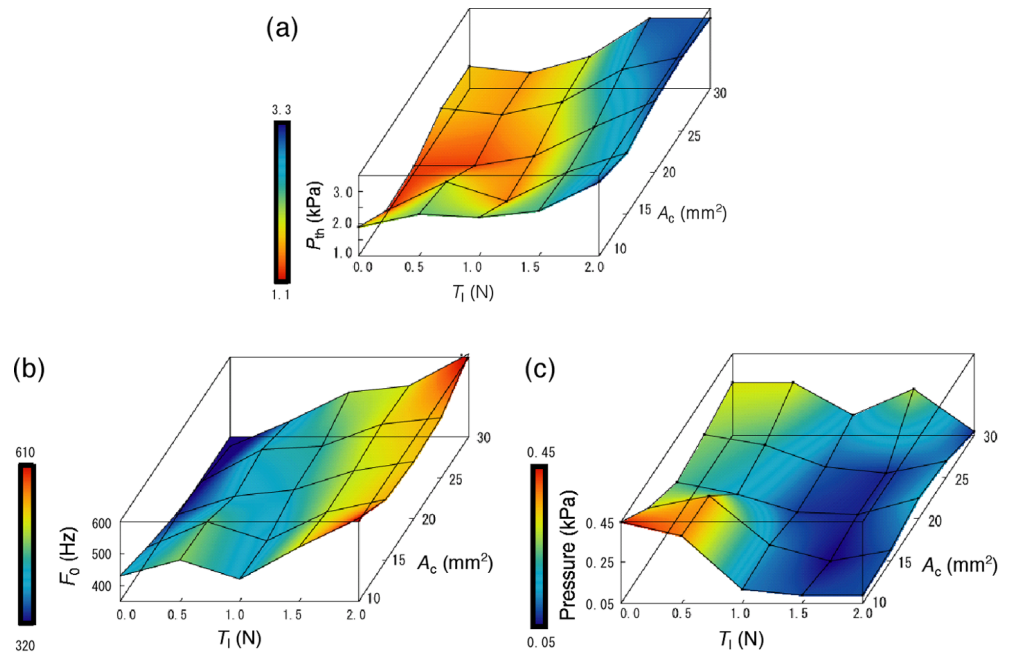
Fig. 4 Measured indexes of the oscillation threshold as a function of T_l and A_c. (a) P_{th}. (b) F_0 of P_c just after the oscillation onset. (c) Standard deviation of P_c just after the oscillation onset.

kPa at the combination of a higher T_l and a higher A_c, while a smaller value of ~1.1 kPa at the combination of a lower T_l and a moderate value of A_c. Local minimal values of P_{th} as a function of A_c are seen for each tension level, which is in particular more notable in the lower tension range. Fundamental frequency of the rubber sheet oscillation F_0, which is equal to that of the produced sound, was examined by an FFT analysis for 10 pitches of the sound waveforms just after the oscillation onset (Fig. 4b). The lowest value of 320 Hz was obtained at the combination of the lowest T_l of 0.0 N and the largest A_c of 30 mm^2. Meanwhile, the largest value of 610 Hz was obtained at the combination of the largest T_l of 2.0 N and the largest A_c of 30 mm^2. Standard deviation of the pressure fluctuation of the rubber sheet oscillation was also examined for 10 pitches of the sound waveforms just after the oscillation onset to assess magnitude of oscillation amplitude or intensity of the sound (Fig. 4c). A lower value of ~0.07 kPa was obtained at the combination of the largest T_l of 2.0 N and the lowest A_c of 10 mm^2. Meanwhile, the largest value of 0.45 kPa was obtained at the combination of the lowest T_l of 0.0 N and the lowest A_c of 10 mm^2.

3.2 Deformation pattern

A sound produced by the rubber oscillation was detected by the microphone. The electric circuit sent a pulse wave voltage to the controller of the high-speed camera when the detected sound voltage had grown to reach a pre-set value (Fig. 5). The sequential images captured before and after the instant of the receipt of the pulse wave were extracted, which exhibits the behavior of the rubber sheet at the onset of the oscillation. The video movie obtained at the combination of 0.0-N T_l and 30-mm^2 A_c demonstrated that a small-amplitude oscillation occurs locally around the minimum gap region (Fig. 6a). The oscillation gradually grows larger and spreads over the entire rubber sheets. The oscillation pattern is a wavelike motion (Fig. 6b): the front and the posterior portions of the rubber sheet do not move in phase. Specifically, the front moves ahead of the posterior in the direction of overall movement, which is similar with the pattern seen in the actual human vocal fold movement [2]. The observation of the *X-Y* plane using the camera placed at the flow path exit clearly shows that the small-amplitude oscillation is kept without collision, indicating that the oscillation may be developed because of the oscillatory divergence
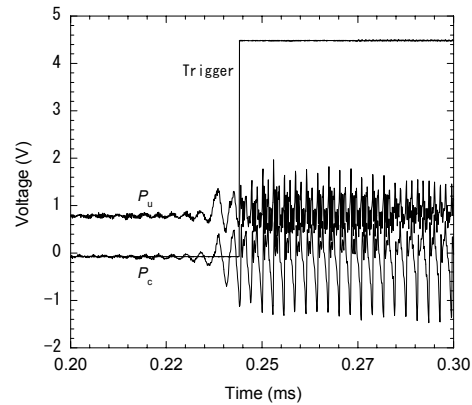
Fig. 5   Microphone and trigger pulse outputs.

mechanism (or flutter) but not the unidirectional divergence mechanism (Fig. 6c). The oscillatory pattern at the onset of the 2.0-N T_1 and 30-mm^2 A_c combination, as a typical result of the high-tension condition, shows that the small-amplitude oscillation is not able to spread out and stays locally at the minimum gap region because the restoring force in the rubber sheet is so strong (Fig. 7). The oscillatory pattern at the onset of the 0.0-N T_1 and 10-mm^2 A_c combination, as a typical result of the small-width condition, shows that large deformation of the rubber sheets is prevented because of the small initial width (Fig. 8).

4. Discussion

The most significant finding of this study using a mechanical vocal fold model is that a small-amplitude oscillation is produced in a part of a flexible wall owing to interaction with a flow and is gradually developed to be a large-amplitude oscillation that spreads out over the wall (Fig. 6). In addition, the magnitude and spreading range of the wall motion seen at the instant of the oscillation initiation is restricted by either increase in wall restoring force (Fig. 7) or narrowness in flow path width (Fig. 8). The pressure measurement experiments of this study suggest that the magnitude and range of the oscillation may be associated with magnitude of P_{th} (Fig. 4a). More specifically, either the high-tension or the small-width reduces degree of oscillation, which limits flow-structure interaction and accordingly enlarges P_{th}, namely a model of the minimum lung pressure and the index of difficulty of phonation. At low-tension or moderate-width range, in contrast, the mechanical vocal fold model provokes a large wavelike motion throughout its body, yielding low values of P_{th}. Over-broadening of the initial width may lower the flow-structure interaction, yielding local minimal values of P_{th} versus A_c particularly at lower tension ranges where the tension effect is weaker. Thus, the present study highlights close association between degrees of oscillation, flow-tissue interaction, and P_{th}.

It is likely that the effects of the two parameters, T_1 and A_c, on the mechanism of the oscillation initiation are analogous to the effects of laryngeal muscles regulating tension in the actual vocal folds and the glottal width on the self-excited oscillation in phonation. In humans, P_{th} has been reported to be ~1 kPa and raised with increases in F_0 [7]. This tendency is seen in the present study when comparing the results of Figs. 4a and 4b, which show some similarity between P_{th} and F_0. The oscillation degree-dependent difficulty of phonation described in the above paragraph may account for the reason of the voice pitch-dependent change in P_{th}. This tendency is also consistent with the distribution of the standard deviation of P_c fluctuation (Fig. 4c) that is an index of the sound intensity or degree of oscillation.

Importantly, an oscillatory divergence without collisions was seen in the process of the oscillation onset (Fig. 6a). This result indicates that the self-excitation occurs owing to an aerodynamic effect in which the energy is transferred from the airflow to the structure. To

understand the mechanism, elucidation of the relation between the driving pressure P_c and the rubber sheet displacement during the process with an F_0 of >100 Hz is required, which will need a difficult experiment and be the subject of future investigation. The result of Fig. 2 exposes a problem to this end, which is typical for and a difficult point of flow-structure interaction as follows: the original constriction position X_c is somewhat displaced after a pressure loading. Hence, P_c that is measured at the original constriction point becomes different from a principal driving pressure acting on the actual constriction point. Considerable modification of the existing experimental setup will be required to enable pressure measurements at arbitrary points in the constriction in addition to theoretical approaches to the problem including stability analyses.
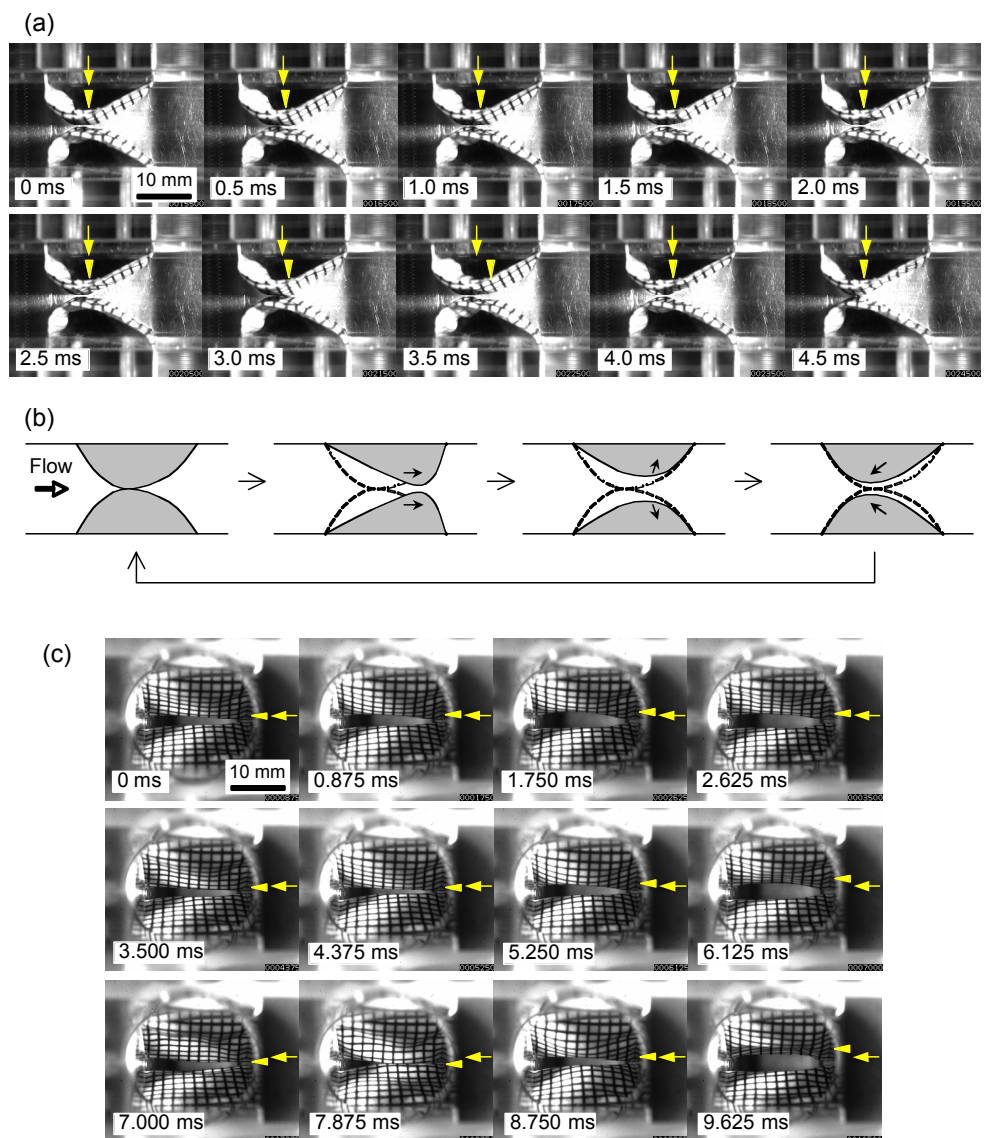

Fig. 6   Sequential images of the oscillation at $T_1 = 0.0$ N and $A_c = 30$ mm^2 taken by the high-speed camera. (a) Approximately two cycles of the oscillation in the *X-Z* plane. Arrowheads indicate the identical point, whose original position is shown by an arrow. (b) Schematic drawing of the wavelike motion depicted exaggeratedly. (c) Approximately three cycles of the oscillation in the *Y-Z* plane. Arrowheads indicate the identical point of the constriction, whose original position is shown by an arrow. Grids of a 2-mm interval are drawn on the rubber sheets to obtain deformation details.
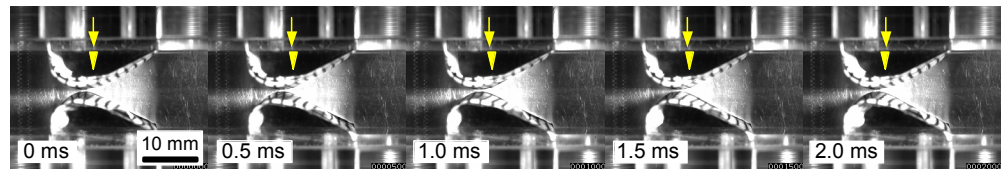
Fig. 7   Sequential images of an approx. single cycle of the fully developed oscillation in the *X-Z* plane at T_1 = 2.0 N and A_c = 30 mm^2. Arrowheads indicate the identical point, whose original position is shown by an arrow.
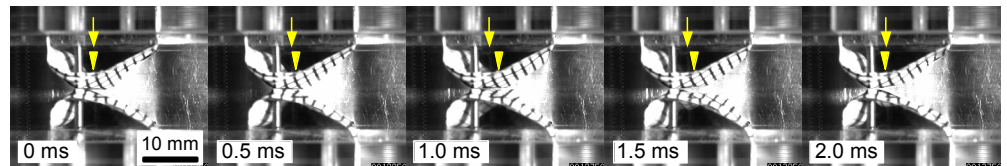

Fig. 8   Sequential images of an approx. single cycle of the fully developed oscillation in the *X-Z* plane at T_1 = 0.0 N and A_c = 10 mm^2. Arrowheads indicate the identical point, whose original position is shown by an arrow. A pair of bolts were mounted to regulate the initial flow path width.

5. Conclusion

We developed a mechanical vocal fold model that enables observation of a high-speed deformation of the vocal fold model, together with pressure measurement. The experiments were focused on the onset of the self-excited oscillation of the vocal fold model because its better understanding has clinical significance in determining the ease with which phonation can be achieved. The observation revealed a gradually developed wavelike oscillation that finally spread out over the vocal fold model. The amplitude and spreading range of the motion (i.e., an index of degrees of flow-structure interaction) was restricted by either increase in restoring force in the vocal fold model or decrease in initial flow path width, each of the effects imitates the actual laryngeal muscle functions. The pressure measurement experiments obtained the threshold upstream pressure required for inducing the onset of the self-excitation. The threshold pressure became higher for the muscle-related experimental parameters that led the lower magnitude of the vocal fold wavelike motion determined from the observations. Thus, the present study highlights close association between degrees of oscillation, flow-tissue interaction, and threshold pressure required for the onset, which may be regulated by laryngeal muscle activations.

References

(1) Ishizaka, K. and Flanagan, J.L., 'Synthesis of Voiced Sounds From a Two-Mass Model of the Vocal Cords', *Bell Syst. Tech. J.*, 51, 1233-1268 (1972).

(2) Eysholdt, T., Tigges, M., Wittenbert, T., and Proschel, U., 'Direct evaluation of high-speed recordings of vocal fold vibrations', *Folia Phoniatr. Logop.*, 48, 163-170 (1996).

(3) Ikeda, T., Matsuzaki, Y., and Aomatsu, T., 'A numerical analysis of phonation using a two-dimensional flexible channel model of the vocal folds', *ASME J. Biomech. Eng.*, 123, 571-579 (2001).

(4) Deguchi, S., Matsuzaki, Y., and Ikeda, T., 'Numerical analysis of effects of transglottal pressure change on fundamental frequency of phonation', *Ann. Otol. Rhinol. Laryngol.*, in press.

(5) Titze, I.R., 'The physics of small-amplitude oscillation of the vocal folds', *J. Acoust.*

Soc. Am. 83, 1536-1552 (1988).

(6) Farley, G.R., 'A quantitative model of voice F_0 control', *J. Acoust. Soc. Am.*, 95, 1017-1029 (1994).

(7) Verdolini-Marston, K., Titze, I.R., and Druker, D.G., 'Changes in phonation threshold pressure with induced conditions of hydration', *J. Voice*, 4, 142-151 (1990).

(8) Titze, I.R., Schmidt, S.S., and Titze, M.R., 'Phonation threshold pressure in a physical model of the vocal fold mucosa', *J. Acoust. Soc. Am.*, 97, 3080-3084 (1995).

(9) Chan, R.W., Titze, I.R., and Titze, M.R., 'Further studies of phonation threshold pressure in a physical model of the vocal fold mucosa', *J. Acoust. Soc. Am.*, 101, 3722-3727 (1997).

(10) Deguchi, S., Ishimaru, Y. Washio, S., 'Laryngo-stroboscopy for observation of pathological vocal fold oscillation', *Trans. Jpn. Soc. Med. Biol. Eng.*, 43, 709-716 (2005).